Time of Arrival Estimation for UWB Localizers in Realistic Environments

Chiara Falsi,[1] Davide Dardari,[2] Lorenzo Mucchi,[3] and Moe Z. Win[4]

[1] *Dipartimento di Elettronica e Telecomunicazioni, Università degli studi di Firenze, Via Santa Marta 3, 50139 Firenze, Italy*

[2] *The WiLAB, IEIIT/CNR, CNIT, Università di Bologna, Via Venezia 52, 47023 Cesena, Italy*

[3] *Dipartimento di Elettronica e Telecomunicazioni, CNIT, Università degli studi di Firenze, Via Santa Marta 3, 50139 Firenze, Italy*

[4] *Laboratory for Information and Decision Systems (LIDS), Massachusetts Institute of Technology, Room 32-D658, 77 Massachusetts Avenue, Cambridge, MA 02139, USA*

This paper investigates time of arrival (ToA) estimation methods for ultra-wide bandwidth (UWB) propagation signals. Different algorithms are implemented in order to detect the direct path in a dense multipath environment. Different suboptimal, low-complex techniques based on peak detection are used to deal with partial overlap of signal paths. A comparison in terms of ranging accuracy, complexity, and parameters sensitivity to propagation conditions is carried out also considering a conventional technique based on threshold detection. In particular, the algorithms are tested on experimental data collected from a measurement campaign performed in a typical office building.

1. INTRODUCTION

There has been great interest in ultra-wide bandwidth technology in recent years because of its potential for a large number of applications. A large body of literature exists on the characterization of indoor propagation channels and many indoor propagation measurements have been made [1–7]. Due to its fine delay resolution properties, UWB shows good capability for short-range communications in dense multipath environments. One of the most attractive capabilities of UWB technology is accurate position localization [8–10]. The transmission of extremely short pulses or equivalently the use of extremely large transmission bandwidths provides the ability to resolve multipath components. This implies high ranging accuracy.

Position estimation is mainly affected by noise, multipath components, and different propagation speeds through obstacles in non-line-of-sight (NLOS) environments. Most positioning techniques are based on the time of arrival (ToA) estimation of the first path [11]. Generally, the first path is not the strongest, making the estimation of the ToA challenging in dense multipath channels.

ToA estimation in a multipath environment is closely related to channel estimation, where channel amplitudes and time of arrivals are jointly estimated using, for example, a maximum likelihood (ML) approach [12, 13]. Received paths often partially overlap and thus become unresolvable, thereby degrading the ToA estimation. This situation is considered in [14] where an ML delay acquisition algorithm for code division multiple access (CDMA) systems in nonresolvable channels is proposed. First, distinct path packets are located using a conventional acquisition algorithm to reduce the set of possible delay combinations to be tested, then the mean squared error between the received signal and a set of hypothesized estimated signals is minimized. In [15] a generalized ML-based ToA estimation is applied to UWB signals, by assuming that the strongest path is perfectly locked and estimating the relative delay of the first path using statistical models based on experimental data.

The problem of estimating the channel parameters can be considered a special case of the harmonic retrieval problems that are well studied in spectral estimation literature. There is a particularly attractive class of subspace or SVD-based algorithms, called high-resolution methods, which can resolve closely spaced sinusoids from a short record of noise-corrupted data. An example is given by the root multiple signal classification (MUSIC) [16], which uses the noise whiteness property to identify the signal subspace from an eigenvalue decomposition of the received signal correlation matrix. For CDMA systems the MUSIC super-resolution algorithm is applied in [17] to frequency-domain channel measurement data to obtain the ToA estimation in indoor WLAN scenarios. In [18] a scheme for the detection of the first arriving path using the generalized likelihood ratio test (GLRT)

in a multipath environment in severe NLOS conditions is described, and a high-resolution ToA estimation algorithm using minimum variance (MV) and normalized minimum variance (NMV) is proposed. In [19] several frequency-domain methods are proposed for UWB channel estimation and rapid acquisition. In particular, the problem of low-complexity channel estimation and timing synchronization in UWB systems using low sampling rates and low power consumption methods is addressed. In [20] we demonstrate how the presence of multipath can be used to reduce the acquisition time.

Methods for calibration and mitigation of NLOS ranging errors are analyzed in [21, 22] and, in the specific UWB range estimation context, in [23]. An algorithm for ranging estimation in the case of an intermittently blocked LOS is proposed in [24].

Most of these works rely on simulation results and have not been verified with actual experimental data. In addition, the propagation conditions for which a specific ToA estimation technique result to be more convenient from the complexity-accuracy compromise point of view with respect to a simpler method (e.g., the conventional one based on threshold detection) have not yet been investigated. Moreover, the previous literature has mainly focused on the effect of NLOS propagation on ranging accuracy. In the case of no high ranging accuracies are required, lower complexity ToA estimators can be considered such as those based on energy detection [25, 26].

The main purpose of our work is to investigate the effects of multipath propagation on ToA estimation using real measurement data by considering different algorithms with different levels of complexity. The trade-off between estimation accuracy, complexity and sensitivity to parameter choice for different propagation conditions is discussed.

Due to the large number of paths characterizing typical UWB propagation environments, the complexity of system implementation of super-resolution techniques can be prohibitive. On the other hand, the ML criterion for channel estimation requires a multidimensional optimization of a highly oscillatory error function, implying a huge, complex computational solution. For these reasons, we evaluate the performance of suboptimal ToA algorithms with increasing levels of complexity derived from the ML criterion and based on a simple peak detection process. In particular, we propose a novel estimation strategy able to cope with the presence of unresolvable multipath, called *search subtract and readjust*. The performance of a conventional technique based on threshold detection is investigated as well, to better understand the conditions for which the adoption of more complex techniques results to be convenient.

It is known [27] that the presence of noise and multipath creates ambiguities in the ToA estimate, mainly because the direct path is not always the strongest one. In this paper we will show two fundamental consequences; a noticeable bias and a significant variance are introduced on the ToA estimate. As we will show later, in some propagation conditions a good channel estimator does not necessarily give

significant gains in the ToA estimation of the direct path, hence the price for the increased complexity may not be justifiable. Additionally, some discussion on NLOS excess propagation delay is presented, showing that its effects would not be always dominant with respect to the effects of multipath if the ToA estimation scheme parameters are not optimized.

This paper is organized as follows. Section 2 provides the theoretical background from which the multipath estimator is derived. Section 3 describes the proposed algorithms and their implementation. The performance of the proposed algorithms is given in Section 4. Section 5 concludes the paper.

2. MULTIPATH ESTIMATOR

2.1. System model

We consider a multipath channel with an impulse response given by

$$c(t) = \sum_{l=1}^{L} c_l \delta(t - \tau_l), \qquad (1)$$

where c_l and τ_l, respectively, are the amplitudes and time delays of the L propagation paths.

In this case, the received signal can be expressed as

$$r(t) = \sum_{l=1}^{L} c_l w(t - \tau_l) + n(t), \qquad (2)$$

where $w(t)$ is the isolated ideal received pulse with duration T_p (i.e., in the absence of multipath and noise) and $n(t)$ is additive white Gaussian noise (AWGN) with zero mean and spectral density $N_0/2$.

We are interested in the estimation of τ_1, that is, the ToA of the direct path, when it exists, based on the observation of the received signal in the interval $[0, T]$. However, due to the presence of multipath, the received waveform depends on a set of unknown parameters, denoted by $\mathcal{U} = \{\boldsymbol{\tau}, \mathbf{c}\}$, where $\boldsymbol{\tau} \triangleq [\tau_1, \tau_2, \ldots, \tau_L]^T$ and $\mathbf{c} \triangleq [c_1, c_2, \ldots, c_L]^T$. Note that the ToA estimation is closely related to the problem of channel estimation, where not only τ_1 but the entire set of unknown parameters is estimated.

This work relies on data collected in a UWB propagation experiment, thus the system is characterized by sampled signals. The transmitted and received signals are composed of Z and M samples ($Z < M$), respectively, at the sampling rate $1/T_s$, such that $T = M \cdot T_s$ and $T_p = Z \cdot T_s$. In this situation, the received signal can be written in vector form as follows:

$$\mathbf{r} = \mathbf{W}(\boldsymbol{\tau})\mathbf{c} + \mathbf{n}, \qquad (3)$$

where

$$\boldsymbol{n} \in \mathbb{R}^M \text{ with elements } n_i = n(iT_s), \quad \text{for } i = 1, 2, \ldots, M,$$

$$\boldsymbol{r} \in \mathbb{R}^M \text{ with elements}$$

$$r_i = r(iT_s)$$

$$= \sum_{l=1}^{L} c_l w(iT_s - \tau_l) + n(iT_s), \quad \text{for } i = 1, 2, \ldots, M,$$

$$\boldsymbol{W}(\boldsymbol{\tau}) = [\boldsymbol{w}^{(D_1)}, \boldsymbol{w}^{(D_2)}, \ldots, \boldsymbol{w}^{(D_L)}] \in \mathbb{R}^{M \times L}. \tag{4}$$

In the previous expression

$$\boldsymbol{w}^{(D_l)} = [\boldsymbol{0}_{D_l}, \boldsymbol{w}, \boldsymbol{0}_{M-Z-D_l}]^T \in \mathbb{R}^M, \quad \text{for } l = 1, 2, \ldots, \tag{5}$$

where

$$\boldsymbol{w} \in \mathbb{R}^Z \text{ with elements } w_i = w(iT_s), \quad \text{for } i = 1, 2, \ldots, Z,$$

$$\boldsymbol{0}_{D_l} = [\underbrace{0, \ldots, 0}_{D_l}],$$

$$\boldsymbol{0}_{M-Z-D_l} = [\underbrace{0, \ldots, 0}_{M-Z-D_l}] \tag{6}$$

and D_l is the discretized version of time delay τ_l, such that $\tau_l \simeq D_l \cdot T_s$. It is worth noting that L columns of matrix $\boldsymbol{W}(\boldsymbol{\tau})$ represent sampled replicas of $w(t)$ shifted by delays τ_l for $l = 1, \ldots, L$ where $0 < \tau_1 < \tau_2 < \cdots < \tau_L$ and $\max_l\{\tau_l\} \leq T - T_p$.

2.2. ML estimator

When the observation noise is Gaussian, the ML criterion is equivalent to the minimum mean squared error (MMSE) criterion. Thus, given an observation $\boldsymbol{r}$ of the received signal, the ML estimates of the delay vector $\boldsymbol{\tau}$ and amplitude vector $\boldsymbol{c}$ are the values that minimize the following mean squared error:

$$S(\boldsymbol{\tau}, \boldsymbol{c}) = \frac{1}{M} \sum_{i=1}^{M} |r_i - \hat{r}_i|^2, \tag{7}$$

where

$$\hat{r}_i = \hat{r}(iT_s) = \sum_{l=1}^{L} c_l w(iT_s - \tau_l), \quad \text{for } i = 1, 2, \ldots, M, \tag{8}$$

is the reconstructed discrete-time signal, based on the set of parameters $\mathcal{U}$. It can be shown that the ML estimates of $\boldsymbol{\tau}$ and $\boldsymbol{c}$ in the continuous-time domain, here reformulated in the discrete-time domain, are given by [12]

$$\hat{\boldsymbol{\tau}} = \arg\max_{\boldsymbol{\tau}} \{\boldsymbol{\chi}^T(\boldsymbol{\tau}) \boldsymbol{R}_w^{-1}(\boldsymbol{\tau}) \boldsymbol{\chi}(\boldsymbol{\tau})\},$$
$$\hat{\boldsymbol{c}} = \boldsymbol{R}_w^{-1}(\hat{\boldsymbol{\tau}}) \boldsymbol{\chi}(\hat{\boldsymbol{\tau}}), \tag{9}$$

where

$$\boldsymbol{\chi}(\boldsymbol{\tau}) = \boldsymbol{W}^T(\boldsymbol{\tau})\boldsymbol{r} = [\boldsymbol{w}^{(D_1)^T}\boldsymbol{r}, \boldsymbol{w}^{(D_2)^T}\boldsymbol{r}, \ldots, \boldsymbol{w}^{(D_L)^T}\boldsymbol{r}] \in \mathbb{R}^L \tag{10}$$

is the correlation between the received signal and different delayed versions of $w(t)$ and

$$\boldsymbol{R}_w(\boldsymbol{\tau})$$
$$= \boldsymbol{W}^T(\boldsymbol{\tau})\boldsymbol{W}(\boldsymbol{\tau})$$
$$= \begin{bmatrix} \boldsymbol{w}^{(D_1)^T}\boldsymbol{w}^{(D_1)} & \boldsymbol{w}^{(D_1)^T}\boldsymbol{w}^{(D_2)} & \cdots & \boldsymbol{w}^{(D_1)^T}\boldsymbol{w}^{(D_L)} \\ \boldsymbol{w}^{(D_2)^T}\boldsymbol{w}^{(D_1)} & \boldsymbol{w}^{(D_2)^T}\boldsymbol{w}^{(D_2)} & \cdots & \boldsymbol{w}^{(D_2)^T}\boldsymbol{w}^{(D_L)} \\ \vdots & \vdots & \ddots & \vdots \\ \boldsymbol{w}^{(D_L)^T}\boldsymbol{w}^{(D_1)} & \boldsymbol{w}^{(D_L)^T}\boldsymbol{w}^{(D_2)} & \cdots & \boldsymbol{w}^{(D_L)^T}\boldsymbol{w}^{(D_L)} \end{bmatrix} \in \mathbb{R}^{L \times L} \tag{11}$$

is the autocorrelation matrix of $w(t)$. Hence (9) can be rewritten as

$$\hat{\boldsymbol{\tau}} = \arg\max_{\boldsymbol{\tau}} \left\{ (\boldsymbol{W}^T(\boldsymbol{\tau})\boldsymbol{r})^T (\boldsymbol{W}^T(\boldsymbol{\tau})\boldsymbol{W}(\boldsymbol{\tau}))^{-1} \boldsymbol{W}^T(\boldsymbol{\tau})\boldsymbol{r} \right\}, \tag{12}$$

$$\hat{\boldsymbol{c}} = \underbrace{(\boldsymbol{W}^T(\hat{\boldsymbol{\tau}})\boldsymbol{W}(\hat{\boldsymbol{\tau}}))^{-1} \boldsymbol{W}^T(\hat{\boldsymbol{\tau}})}_{\text{pseudo-inverse matrix}} \boldsymbol{r}. \tag{13}$$

When the channel is not separable, that is,

$$|\tau_i - \tau_j| < T_p, \quad \text{for some } i \neq j, \tag{14}$$

we note from (9) that the estimation of the ToA of the direct path, in general, can depend strongly on the estimation of the other channel parameters. Direct optimization of (9) can be computationally complex, since it requires the evaluation of (12) and (13) for each set of hypothesized values of $\hat{\boldsymbol{\tau}}$. It could also be highly oscillatory, that is, (12) involves the hard task of the maximization, over all possible sets of hypothesized values of $\hat{\boldsymbol{\tau}}$, of a multidimensional nonlinear function with several potential local maxima. In Section 3 we propose two possible suboptimal optimization strategies with lower complexity.

On the other hand, when the channel is separable, that is, when

$$|\tau_i - \tau_j| \geq T_p \quad \forall i \neq j, \tag{15}$$

the expressions (9) are simplified to

$$\hat{\boldsymbol{\tau}} = \arg\max_{\tau_l} \left\{ \sum_{l=1}^{L} \frac{[\chi(\tau_l)]^2}{R_w(0)} \right\} = \arg\max_{\tau_l} \left\{ \sum_{l=1}^{L} \frac{[\boldsymbol{w}^{(D_l)^T}\boldsymbol{r}]^2}{E_w} \right\}, \tag{16}$$

$$\hat{\boldsymbol{c}} = \frac{\chi(\hat{\boldsymbol{\tau}})}{R_w(0)} = \frac{\boldsymbol{W}^T(\hat{\boldsymbol{\tau}})\boldsymbol{r}}{E_w}, \tag{17}$$

where $R_w(0) = E_w$ is the energy of $w(t)$. In this case the estimation of the ToA of the direct path is decoupled from the estimation of the other channel parameters, that is, optimization of (16) can be accomplished by maximizing each term of the sum independently.

It can be seen from (10) that the system can be implemented with the discrete-time version of matched filters. In fact, each element of $\boldsymbol{\chi}(\boldsymbol{\tau})$ is the discrete correlation between

the received signal and a different delayed version of $w(t)$. As a result, (16) can be simply accomplished observing the MF output at proper instants. The discrete-time impulse response of the MF is

$$\boldsymbol{h} = \left[w(ZT_s), w((Z-1)T_s), \ldots, w(T_s) \right]^T \in \mathbb{R}^Z, \quad (18)$$

and the sampled output of the MF can be written as the discrete convolution ($*$) between the impulse response of the MF ($\boldsymbol{h}$) and the received signal ($\boldsymbol{r}$) as follows:

$$\boldsymbol{y} = \boldsymbol{h} * \boldsymbol{r} \text{ with elements },$$
$$y_i = \sum_{j=1}^{Z} h_j r_{i-j+1}, \quad \text{for } i = Z, Z+1, \ldots, M. \quad (19)$$

Under condition (15), and considering a transmitted pulse without sidelobes, in the absence of noise, the values τ_l with $l = 1, 2, \ldots, L$ could be easily found from the locations t_l of the peaks of the MF output, since $\tau_l = t_l - T_p$. It is worth noting that the parameter we are interested in for the purpose of ranging is τ_1, which is the smallest element in the vector $\hat{\boldsymbol{\tau}}$, that is, the path that arrives first among all the detected paths.

In the presence of noise, and in a more realistic situation where the autocorrelation of $w(t)$ has non-negligible sidelobes, it becomes more challenging to recognize the correct signal peaks at the MF output. In Section 3 we suggest two different solutions for selecting the location of the peaks as the best values of the ToAs in order to achieve a high ranging accuracy.

3. ESTIMATION STRATEGIES

3.1. Peak-detection-based estimator

We consider three algorithms based on peak detection, called *single search*, *search and subtract* and *search, subtract and readjust*. As the following will make clear, they are characterized by an increasing level of complexity. These algorithms essentially involve the detection of N largest positive and negative values of the MF output, where the parameter N is the number of paths considered in the search by the algorithms, and the determination of the corresponding time locations $t_{k_1}, t_{k_2}, \ldots, t_{k_N}$. While these algorithms are equivalent, that is, give the same delay and amplitude estimates, when the multipaths are separable, the last two algorithms take into account the effects of a nonseparable channel.

3.1.1. Single search

The delay and amplitude vectors are estimated with a single look.

(a) Calculate the MF output using (19).
(b) Given the absolute value $\boldsymbol{v} = |\boldsymbol{y}|$ of the MF output, find N samples v_{k_i}, with $i = 1, 2, \ldots, N$, corresponding to both positive and negative N largest peaks of $\boldsymbol{y}$.
(c) Convert the indexes k_i into the time locations $t_{k_i} = k_i \cdot T_s$ of the peaks and from them derive the delay

estimates $\hat{\tau}_{k_i} = t_{k_i} - T_p$. Then find the minimum of $\{\hat{\tau}_{k_i}\}_{i=1}^N$ and set it as the delay estimate $\hat{\tau}_1$ of the ToA of the direct path.

3.1.2. Search and subtract

This algorithm provides a way to detect multipath components in a nonseparable channel.

(a) Calculate the MF output using (19).
(b) Find the sample v_{k_1} corresponding to the largest peak of the absolute value of the MF output, convert the index into the corresponding time location $t_{k_1} = k_1 \cdot T_s$, and then derive the delay estimate $\hat{\tau}_{k_1} = t_{k_1} - T_p$ of the strongest path, which does not necessarily coincide with the first path.
(c) Calculate the amplitude estimate $\hat{c}_{k_1}$ of the strongest path solving (13), which gives

$$\hat{c}_{k_1} = \left(\boldsymbol{w}^{(k_1)^T} \boldsymbol{w}^{(k_1)} \right)^{-1} \boldsymbol{w}^{(k_1)^T} \boldsymbol{r}. \quad (20)$$

(d) Subtract out the estimated path from the received vector $\boldsymbol{r}$ and calculate the new observation signal $\boldsymbol{r}'$ as follows: $\boldsymbol{r}' = \boldsymbol{r} - \hat{c}_{k_1} \boldsymbol{w}^{(k_1)}$.
(e) Calculate the following discrete convolution: $\boldsymbol{y}' = \boldsymbol{h} * \boldsymbol{r}'$; find the sample v'_{k_2} corresponding to the largest peak of the absolute value of the new MF output, then convert the index into the corresponding time location $t_{k_2} = k_2 \cdot T_s$, and derive the delay estimate $\hat{\tau}_{k_2} = t_{k_2} - T_p$ of the second strongest path of $\boldsymbol{r}$.
(f) Estimate the corresponding amplitude $\hat{c}_{k_2}$ using (13), which is now equal to

$$\hat{c}_{k_2} = \left(\boldsymbol{w}^{(k_2)^T} \boldsymbol{w}^{(k_2)} \right)^{-1} \boldsymbol{w}^{(k_2)^T} \boldsymbol{r}. \quad (21)$$

(g) Subtract out the estimated path from $\boldsymbol{r}'$, obtaining $\boldsymbol{r}'' = \boldsymbol{r}' - \hat{c}_{k_2} \boldsymbol{w}^{(k_2)}$.
(h) Repeat the same process until the N strongest paths are found. Then find the minimum of $\{\hat{\tau}_{k_i}\}_{i=1}^N$ and set it as the estimate $\hat{\tau}_1$ of the ToA of the direct path.

3.1.3. Search subtract and readjust

So far the delay and amplitude of each path are estimated separately at each step; in this algorithm a joint estimation of the amplitudes of different paths is introduced.

(a) Calculate the output of the MF, given by (19).
(b) Find the sample v_{k_1} corresponding to the largest peak of the absolute value of the MF output, convert the index into the corresponding time location $t_{k_1} = k_1 \cdot T_s$, and derive the delay estimate $\hat{\tau}_{k_1} = t_{k_1} - T_p$ of the strongest path.
(c) Calculate the amplitude estimate $\hat{c}_{k_1}$ of the strongest path from (13):

$$\hat{c}_{k_1} = \left(\boldsymbol{w}^{(k_1)^T} \boldsymbol{w}^{(k_1)} \right)^{-1} \boldsymbol{w}^{(k_1)^T} \boldsymbol{r}. \quad (22)$$

(d) Subtract out the estimated path from the received vector $\boldsymbol{r}$ and calculate the new observation signal $\boldsymbol{r}'$ as follows: $\boldsymbol{r}' = \boldsymbol{r} - \hat{c}_{k_1} \boldsymbol{w}^{(k_1)}$.

(e) Calculate the discrete convolution between the new observation signal and the MF impulse response as follows: $\boldsymbol{y}' = \boldsymbol{h} * \boldsymbol{r}'$. Find the sample v'_{k_2} corresponding to the largest peak of the absolute value of the new MF output, then convert the index into the corresponding time location $t_{k_2} = k_2 \cdot T_s$ and derive the delay estimate $\hat{\tau}_{k_2} = t_{k_2} - T_p$ of the second strongest path of $\boldsymbol{r}$.

(f) Given $\hat{\tau}_{k_1}$ and $\hat{\tau}_{k_2}$, estimate the corresponding amplitudes of the first two strongest paths of the received signal. This step can be accomplished solving the following equation:

$$
\begin{bmatrix} \hat{c}_{k_1} \\ \hat{c}_{k_2} \end{bmatrix} = \left(\left[\boldsymbol{w}^{(k_1)}, \boldsymbol{w}^{(k_2)} \right]^T \left[\boldsymbol{w}^{(k_1)}, \boldsymbol{w}^{(k_2)} \right] \right)^{-1}
$$
$$
\times \left[\boldsymbol{w}^{(k_1)}, \boldsymbol{w}^{(k_2)} \right]^T \begin{bmatrix} r_1 \\ \vdots \\ r_M \end{bmatrix}. \tag{23}
$$

It is worth noting that, unlike in the *search and subtract* algorithm, here the amplitudes of the paths selected as the strongest are jointly estimated at each step.

(g) Subtract out the two estimated paths from $\boldsymbol{r}$, obtaining $\boldsymbol{r}'' = \boldsymbol{r} - \hat{c}_{k_1} \boldsymbol{w}^{(k_1)} - \hat{c}_{k_2} \boldsymbol{w}^{(k_2)}$.

(h) Repeat the same process until the N strongest paths are found. Then find the minimum of $\{\hat{\tau}_{k_i}\}_{i=1}^N$ and set it as the estimate $\hat{\tau}_1$ of the ToA of the direct path.

In the above three algorithms, the parameter N has to be determined with an optimization process, as will be demonstrated. Moreover, the choice of N also affects the computational complexity of the strategy adopted. In particular, both *search and subtract* and *search subtract and readjust* require a matrix inversion process at each step for a total of N matrix inversions. In the *search subtract and readjust* algorithm the matrix dimension increases by a factor L at each step, thus making its complexity higher than the other strategies considered. It will be shown in the numerical results that reasonable ToA estimation accuracy can be obtained with a low number of steps N. In general the matrix $\boldsymbol{W}(\boldsymbol{\tau})$ is sparse, thus efficient inversion techniques can be utilized. However, a detailed analysis of the complexity issue is out of the scope of this paper. The *single search* strategy does not require complex computational processes (only comparisons and ordering), thus implying a very low complexity.

3.2. Thresholding-based estimator

We now consider the conventional threshold detection algorithm, well known from radar theory [28]. We call it *threshold and search*. ToA estimation involves the following steps.

(a) Pass the received discrete-time signal through the MF and calculate the MF output using (19).

(b) Compare the absolute value $\boldsymbol{v}$ of the MF output $\boldsymbol{y}$ to fixed threshold λ.

(c) After the first threshold crossing point is found (detection), search for the peak in an interval of length T_p (fine estimation); then convert the index of the peak sample v_k to the time location $t_k = k \cdot T_s$, derive the

delay estimate $\tau_k = t_k - T_p$ and set it as the estimate $\hat{\tau}_1$ of the ToA of direct path.

Among the algorithms considered in the paper, this one requires the lowest level of computational complexity since only comparison operations are required, independently on the parameter λ.

The choice of threshold is important. With a small threshold, the probability of detecting peaks due to noise, that is, false alarm, and thus estimating the position of an erroneous path arriving earlier than the actual direct path as $\hat{\tau}_1$ is high. Whereas with a large threshold, the probability of missing the direct path and thus estimating the position of an erroneous path arriving later as $\hat{\tau}_1$, that is, missed detection, is high. We optimized the threshold considering the overall signal dynamics at the MF output over the observation interval T, to obtain the lowest estimation error, as will be explained in the next section.

4. PERFORMANCE ANALYSIS

4.1. A brief description of a UWB propagation experiment

For convenience we briefly review the UWB experiment [12]. The excitation signal of our propagation channel is a pulse with a duration of approximately one nanosecond, implying a bandwidth signal of 1 GHz. A periodic probing pulse with a repetition rate of 2×10^6 pulses per second is used, so that successive multipath components spread up to 500 nanoseconds (ns) can be measured unambiguously. In fact the duration of one pulse, inversely proportional to the transmission bandwidth, determines the minimum differential path delay between resolvable multipath components, while the repetition time of the periodic pulse signal determines the maximum observable multipath dispersion of the channel.

The channel response is recorded using a digital sampling oscilloscope (DSO) with a sampling rate of 20.48 GHz, which means that the time between samples is $T_s = 48.828$ picoseconds (ps) and the measurement apparatus is set in such a way that all the multipath profiles have the same absolute delay reference.

Multipath profiles data are collected in 14 rooms and along the hallways on one floor of the building.[1] In each room the measurements are made at 49 different points located at a fixed height on a 7×7 square grid, covering 90×90 centimeters (cm) with 15 cm spacing between measurement points. Moreover, the transmitted pulse $w(t)$ is measured 1 m apart from the antenna in LOS condition and the observed waveform has been used as a template pulse in the implementation of the algorithms.

We focus our attention on the measured signals from the following four locations.

(i) Room F1, which represents a typical "direct line-of-sight (LOS)" UWB signal transmission environment,

---

[1] A detailed floor plan of the building where the measurement experiment was performed can be viewed in [12].
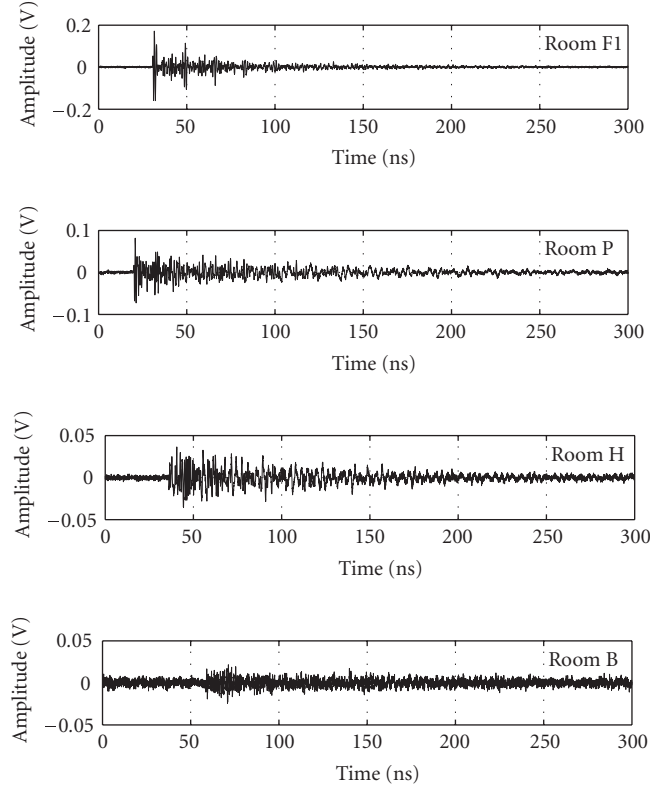
FIGURE 1: Multipath profile measured at the center point (4,4) of the grid in room F1, room P, room H, and room B.

where the transmitter and the receiver are located in the same room without any blockage in between.

(ii) Room P, which represents a typical "high signal-to-noise ratio (SNR)" UWB signal transmission environment. The approximate distance between the transmitter and the receiver is 6 meters.

(iii) Room H, which represents a typical "low SNR" UWB signal transmission environment. The approximate distance between the transmitter and the receiver is 10 meters.

(iv) Room B, which represents a typical "extreme-low SNR" UWB signal transmission environment. The approximate distance between the transmitter and the receiver is 17 meters.

Figure 1 shows some representative examples of the received waveforms measured in the different locations.

4.2. Measurement-based performance analysis

The multipath profiles collected from the $Q = 49$ locations on the measurement grid in each room are processed using algorithms described in Section 3, in order to analyze the variations caused by small changes of the receiver position. For each point i of the grid, we evaluate the error on the estimate of the ToA of the direct path, defined as $\epsilon^{(i)} = \hat{\tau}_1^{(i)} - \tau_1^{(i)}$.

We also obtain the mean and variance of the ToA estimation error averaged over the Q measurement locations inside each room.

(i) The mean value of the ToA estimation error is given by

$$\mu_\epsilon = \frac{1}{Q} \sum_{i=1}^{Q} \epsilon^{(i)}. \tag{24}$$

(ii) The standard deviation of the ToA estimation error is given by

$$\sigma_\epsilon = \sqrt{\frac{1}{Q} \sum_{i=1}^{Q} \left(\epsilon^{(i)}\right)^2 - \mu_\epsilon^2}. \tag{25}$$

4.2.1. Peak-detection-based estimator performance

Figures 2 and 3 show the Q values of $\epsilon^{(i)}$ for *search and subtract* algorithm, as a function of the number of considered paths N for measurements made in different rooms. The line representing the mean of the ToA estimation error is superimposed in the plots, where there are Q crosses (each correspondent to each measurement location) for every value of N. Two regions in the behavior of μ_ϵ can be recognized with respect to the increasing number of considered paths.

(i) When a small number of strongest paths is considered, the first one may not be included, since the first path is not always the strongest. Thus, the direct path is missed and a path arriving later is declared the first path, causing μ_ϵ to assume positive values.
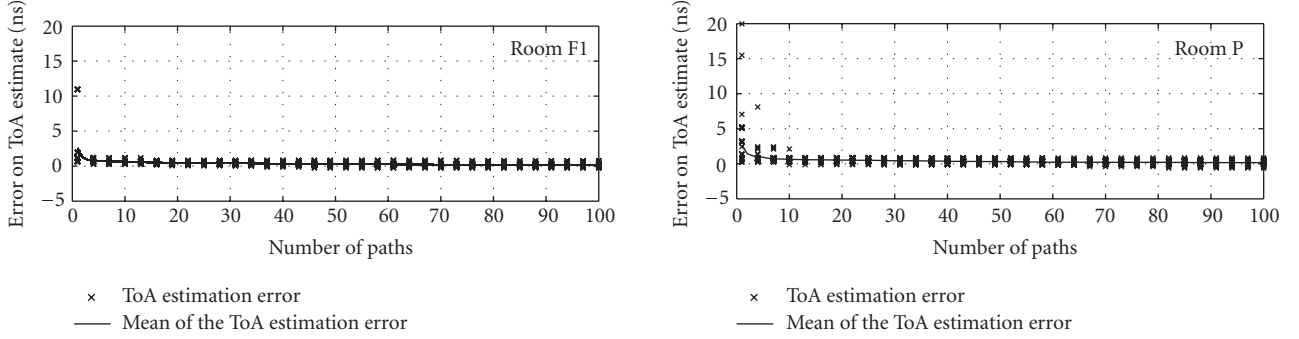
FIGURE 2: ToA estimation error versus number of paths in the 49 points of the grid in rooms F1 and P (crosses) and mean of the ToA estimation error (line). Searh and subtract algorithm was used.
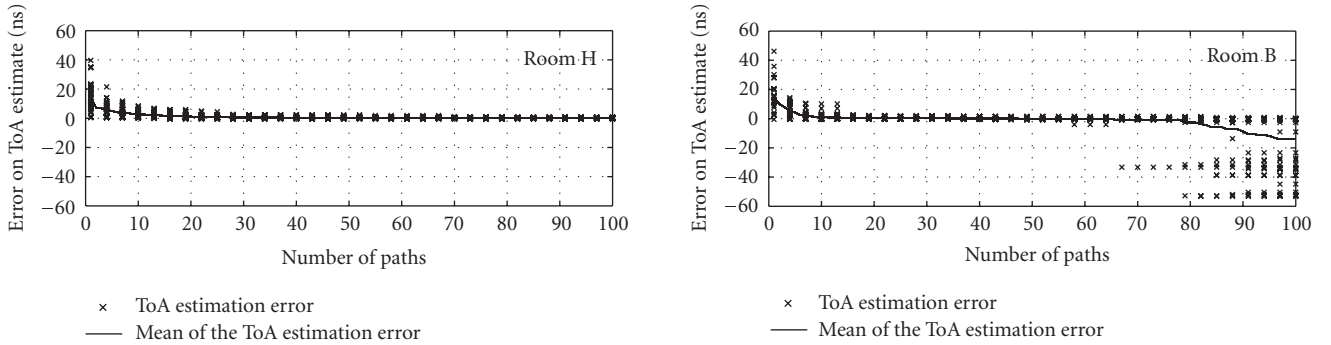

FIGURE 3: ToA estimation error versus number of paths in the 49 points of the grid in rooms H and B (crosses) and mean of the ToA estimation error (line). Search and subtract agorithm was used.

(ii) As the number of considered paths increases, the mean of the ToA estimation error decreases. Especially in the "extreme-low SNR" case with a high number of paths, μ_ϵ keeps decreasing towards negative values since some paths in the noise portion are detected.

In Figure 4 we can see the behavior of the standard deviation of the ToA estimation error in room F1, room P, room H, and room B. It is worth noting that two regions can be recognized again. Initially, σ_ϵ assumes large values, then, as the number N of considered paths increases, σ_ϵ decreases, reaching its minimum. In such situations, where the mean assumes values around zero and the standard deviation assumes the minimum value, an optimum operating point can be defined. The optimum number of paths to be considered corresponds to the value that minimizes the mean squared error (MSE), defined as

$$\mathrm{MSE}_\epsilon = \sigma_\epsilon^2 + \mu_\epsilon^2 \qquad (26)$$

for the ToA estimation error. Unlike all other cases, it can be seen from Figure 5 that in the "extreme-low SNR" case σ_ϵ becomes high when a large number of paths is considered; this happens because room B presents a high noise floor, which makes it easier to detect false paths in the noise portion.

It is worth mentioning that the three algorithms implementing the *peak-detection-based estimator* are originally considered for the estimation of the entire set of parameters $\mathcal{U}$ that characterize the channel. Figure 5 shows their performance in terms of the *energy capture* [12, 29] defined as

$$\mathrm{EC}(\widehat{\boldsymbol{\tau}}, \widehat{\boldsymbol{c}}, N) = 1 - \frac{S(\widehat{\boldsymbol{\tau}}, \widehat{\boldsymbol{c}})}{(1/M) \sum_{i=1}^{M} |r_i|^2}, \qquad (27)$$

where the estimates of the delay and amplitude vectors obtained from the algorithms have been substituted in (7). This quantity represents the fraction of the received signal energy captured by the UWB receiver and gives an idea about the goodness of the channel estimation process. It can be seen from Figure 5 that the performance improves as we move from the *single search* to the *search and subtract* and to the *search subtract and readjust*. Note that the energy capture as a function of the number of single-path signal correlators is interesting for investigating the realization of a UWB selective Rake receiver. However, when the goal is the estimation of the ToA of the direct path, a better result for the channel estimation does not always imply higher accuracy in the ToA estimation. Our analysis shows that the behavior of mean and standard deviation of the ToA estimation error as a function of the number of considered paths is essentially the same
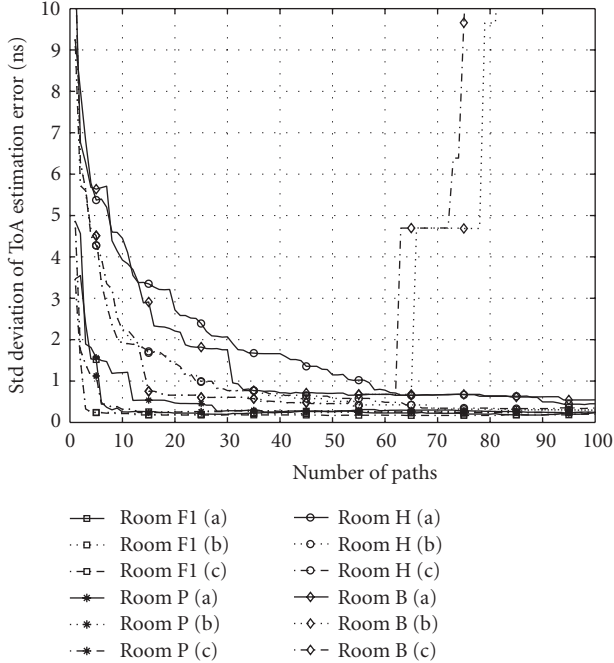
FIGURE 4: Standard deviation of the ToA estimation error versus number of paths in rooms P, H, B, and F1 for the three algorithms: single search (a), search and subtract (b), and search subtract and readjust (c).

in all three algorithms. The *search subtract and readjust* algorithm gives almost exactly the same results as the *search and subtract* in the ToA estimation. The *single search* algorithm, though showing the same general trend for μ_ϵ and σ_ϵ, is better in the "direct LOS" and "high SNR" cases, while it yields worse results in the "low SNR" and "extreme-low SNR" cases.

4.2.2. Thresholding-based estimator performance

Figures 6 and 7 show the Q values $\epsilon^{(i)}$ as a function of the threshold λ for measurements made in different rooms. For every λ in each room there are Q crosses (corresponding to each measurement location). The crosses give an idea of how much the ToA estimation error is spread out around the mean, which is represented by the superimposed line in the plots. Three regions in the behavior of μ_ϵ can be recognized with respect to the increasing threshold.

(i) For small values of λ, similar behaviors of the parameter μ_ϵ can be observed in the different SNR environments. The mean assumes negative values, since there is a high probability that an erroneous path corresponding to noise is estimated as the first arriving path. This phenomenon is clearly stronger in the "low SNR" and "extreme-low SNR" cases; in fact, in the "direct LOS" and "high SNR" cases, the noise floor is negligible, thus the actual direct path is represented by a strong component in the multipath profile, which can be detected with a high probability.
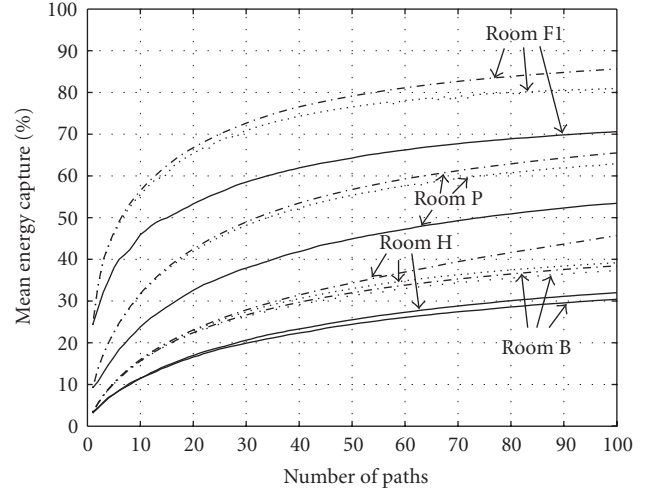

FIGURE 5: Receiver's captured energy averaged on the 49 points of the grid versus number of paths in rooms P, H, B, and F1 for the three algorithms: single search, search and subtract, and search subtract and readjust.

(ii) As the threshold increases, μ_ϵ increases, assuming values around zero.

(iii) For large values of λ, the mean increases under any SNR conditions for the following two reasons: the first path is missed and other paths above the threshold are detected, or no peaks above the threshold are found. In the latter situation, $\hat{\tau}_1$ is set to the time location of the highest peak, which does not always coincide with the first path.

The standard deviation of the ToA estimation error as a function of the ratio λ/ν_{max}, where ν_{max} is the amplitude of the highest peak of the signal over the observation interval T at the MF output, is plotted in Figure 8. It is worth noting that three regions can be recognized again with slight differences among the four environments. The standard deviation is initially small in the "direct LOS" and "high SNR" cases, while it assumes large values in the "low SNR" and "extreme-low SNR" cases; then, as the threshold increases, σ_ϵ decreases, reaching the minimum. In such situations, where the mean assumes values around zero and the standard deviation assumes the minimum value, an optimum operating point can be defined. In fact, the optimum threshold can be determined by choosing the minimum MSE, given by (26). Finally, as λ becomes larger, σ_ϵ increases under any SNR conditions, though it becomes constant when no paths cross the threshold and the time location of the strongest path is chosen for the estimate of $\hat{\tau}_1$.

An important observation can now be made: from Figure 8 we observe that the four curves assume a similar trend, reaching their minimum more or less for the same values of the threshold normalized to the maximum peak. Thus a general criterion for the choice of the optimum threshold
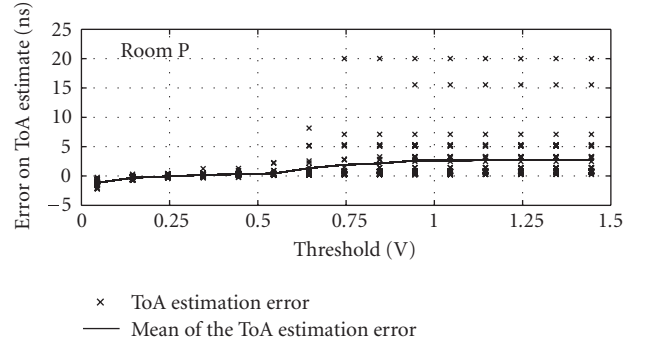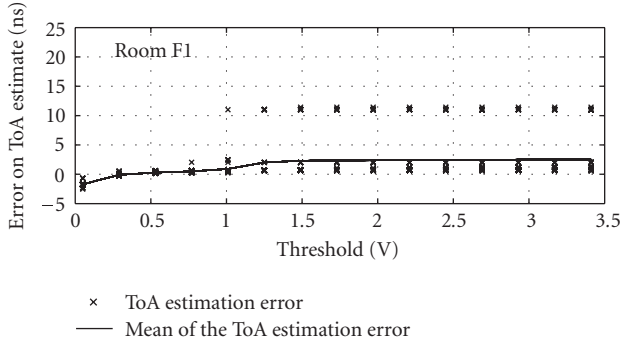
Figure 6: ToA estimation error versus threshold in the 49 points of the grid in rooms F1 and P (crosses) and mean of the ToA estimation error (line).
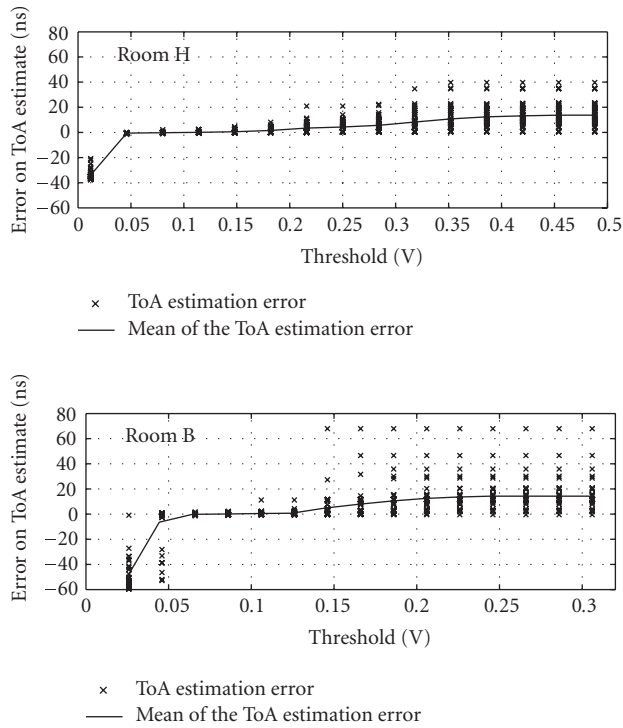

Figure 7: ToA estimation error versus threshold in the 49 points of the grid in rooms H and B (crosses) and mean of the ToA estimation error (line).

Figure 8: Standard deviation of the ToA estimation error on the 49 points of the grid versus threshold in rooms P, H, B, and F1.

is given by the following relationship: $\lambda/v_{\max} \in (0.25, 0.3)$. It can also be seen from Figure 8 that, as the SNR decreases, the choice of the optimum λ becomes constrained within an extremely small interval of values, and thus becomes more critical.

4.3. Ranging accuracy

The evaluation of the ranging accuracy requires the translation of the error on the ToA estimation to the error on the distance estimation, through the following relationships:
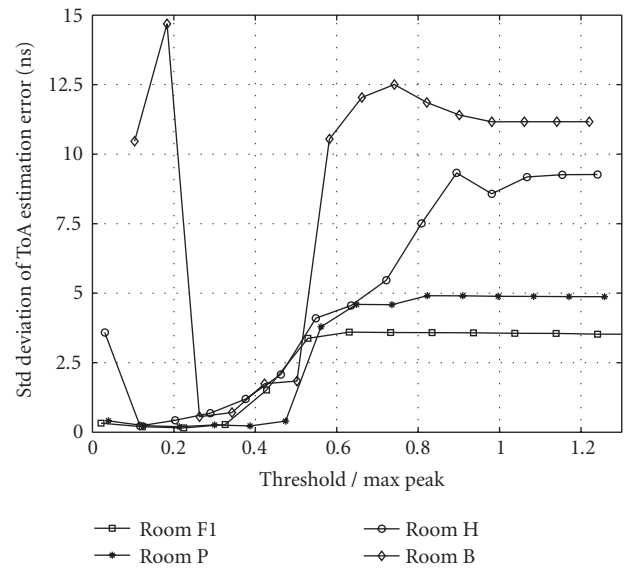
$\sigma_\rho = v \cdot \sigma_\epsilon$ and $\mu_\rho = v \cdot \mu_\epsilon$, where $\rho^{(i)} = \hat{d}^{(i)} - d^{(i)}$ is the error on the distance estimation for each of the Q points i of the grid, and v is the speed of light.

In order to provide a good ToA estimator, it is necessary to minimize mean and standard deviation of the error on the ToA estimate. This objective can be achieved through the optimization of a single parameter in the *thresholding-based estimator*, where we reach for the optimum threshold, and the *peak-detection-based estimator*, where we reach for the optimum number of considered paths. It is worth noting that the evaluation of the optimum threshold is more critical than the choice of the optimum number of considered paths. However, the optimization process is dependent on the context and the application, since it is a trade-off between a small variance and a mean as close to zero as possible. Moreover, it may be convenient, in the *peak-detection-based estimator*, to minimize the number of considered paths in order to obtain a lower computational complexity.

TABLE 1: ToA and distance estimation error in each room for the four algorithms.

Room	Algorithm	μ_ϵ (ns)	σ_ϵ (ns)	μ_ρ (cm)	σ_ρ (cm)	$\mu_\rho/d^{(25)}$ (%)	$\sigma_\rho/d^{(25)}$ (%)
F1 $d^{(25)} = 9.49$ m	Threshold and search	−0.10	0.15	−3.0	5.7	0.32	0.60
	Single search	−0.045	0.19	−1.3	5.7	0.14	0.60
	Search and subtract	0.17	0.24	5.1	7.2	0.54	0.76
	Search subtract and readjust	0.42	0.20	12.6	5.6	1.3	0.59
P $d^{(25)} = 5.77$ m	Threshold and search	−0.082	0.20	−2.46	5.6	0.43	0.97
	Single search	−0.10	0.25	−3.0	7.5	0.52	1.3
	Search and subtract	0.22	0.25	6.6	7.5	1.1	1.3
	Search subtract and readjust	0.24	0.24	7.2	7.2	1.2	1.2
H $d^{(25)} = 10.13$ m	Threshold and search	−0.20	0.43	−5.6	12.9	0.55	1.3
	Single search	−0.38	0.44	−11.4	13.2	1.1	1.3
	Search and subtract	0.11	0.30	3.3	9.0	0.36	0.89
	Search subtract and readjust	0.086	0.34	2.6	10.2	0.26	1.0
B $d^{(25)} = 16.91$ m	Threshold and Search	−0.17	0.56	−5.1	16.8	0.30	0.99
	Single search	−0.19	0.66	−5.7	19.8	0.34	1.2
	Search and subtract	−0.11	0.40	−3.3	12.0	0.20	0.71
	Search subtract and readjust	0.013	0.45	0.39	13.5	0.023	0.80

Table 1 shows the numerical results for the mean and standard deviation of the ToA and distance estimation error obtained from room F1, room P, room H, and room B. It summarizes the performance of the four algorithms at the optimum operating point of the parameters λ and N.

In general, only slight differences can be observed in the performance of the algorithms. However, it is interesting to note that in the "direct LOS" and "high SNR" cases the *threshold and search* and *single search* give better results than the other algorithms; while in the "extreme-low SNR" and "low SNR" cases, the *search and subtract* and *search subtract and readjust* are superior. Thus, when the operating environment is good in terms of SNR, it is sufficient to use the *threshold and search* or the *single search* algorithms, which have very low complexity. However, in an environment with worse SNR conditions, the *search and subtract* and *search subtract and readjust* can be used to reach a reasonable ranging accuracy, in spite of the higher complexity. Moreover, the last two columns of Table 1 show the values of mean and standard deviation of distance estimation error as a fraction of the total distance between the transmitter and the receiver in each room. It can be noted that a slight performance degradation exists when moving from the "direct LOS" case in room F1 to the NLOS cases in the other rooms. However, there is not a noticeable degradation of the ranging accuracy with the increasing distance. In fact, in rooms P, H, and B, where the distance between the transmitter and the receiver is approximately 6 meters, 10 meters, and 17 meters, respectively, the performance of the algorithms in terms of ranging accuracy shows only a negligible degradation. This highlights the fact

that the impact of multipath and walls on the ToA estimation is larger than the SNR loss due to distance.

In order to better analyze the performance of the proposed algorithms with respect to the effects of noise and multipath, the excessive propagation delay, due to blocked LOS conditions, has been subtracted from our ToA estimates. Since the absolute propagation delays of the received signals are different in each room, a delay reference is necessary to analyze the excessive propagation delays. In particular, we calculated the time offset, $\Delta\tau$, between the ideal time of arrival, given by $\tau_1 = d/v$, where d is the distance between the transmitter and the receiver, and the actual time of arrival, given by the time location of the first arriving peak in the received signal, in each room. Then, we assumed the absolute propagation delay of room F1, that is, the delay of the direct LOS path, as the delay reference, taking $\Delta\tau_{F1} = 0$. The following values have been found for the excessive propagation delays of the other rooms: $\Delta\tau_P = 2$ ns, $\Delta\tau_H = 3.7$ ns, and $\Delta\tau_B = 3.7$ ns. Even if the distance between the transmitter and the receiver in room B is larger than in room H, they are characterized by the same $\Delta\tau$, because the number of obstacles is about the same. The results of this work show that the effects of noise and multipath on ranging error could be smaller than those of NLOS propagation delay if the estimator parameters, that is, N in the *peak-detection-based estimator* and λ in the *thresholding-based estimator*, have been optimized. It can be noted from Figures 2–4 and Figures 6–8 that the contribution to the bias in the ToA estimate given by the presence of noise and multipath becomes on the order or greater than that given by the NLOS propagation delay when

the parameters N and λ do not assume the optimum values. The schemes proposed in this paper provide a solution to the problem of reducing the ranging error due to noise and multipath effects, making it smaller than that due to NLOS effects. Moreover, it is worth noting that the choice of the optimum parameters is less critical in the algorithms with a higher complexity.

5. CONCLUSION

A ToA estimation algorithm implementing a conventional threshold-based estimator and three algorithms implementing an ML estimator based on a peak detection process have been studied in this paper using experimental data. Performance analysis underlines the fact that a good channel parameter estimator does not always provide noticeable gains over the conventional threshold-based estimator. The variations in their performance are strongly influenced by the propagation environment; hence, the trade-off between ranging accuracy, algorithm complexity, and sensitivity of the parameters' optimization to propagation conditions becomes an important issue.

For instance, results show that the low complexity threshold-based estimator gives an estimation accuracy close to that obtained using more complex schemes in the case of a high SNR; however, the threshold choice appears much more critical depending on the propagation conditions.

Beyond the numerical values, this paper shows some important results. The presence of noise and multipath generates ambiguities in the ToA estimate, mainly due to the fact that the direct path is not always the strongest one. This has fundamental consequences: a significant bias and variance are introduced in the ToA estimation.

In order to reduce the ToA estimation bias, thereby providing a good ToA estimator, an optimization process of one parameter is necessary. In fact, together with noise, the presence of multipath may lead to a biased ToA estimation even in a high SNR environment, if the threshold (in the *thresholding-based estimator*) or the number of paths (in the *peak-detection-based estimator*) is not properly chosen. In this case, the increased ranging estimation bias may be greater than that produced by the extra propagation delay due to blocked LOS conditions, if present.

ACKNOWLEDGMENTS

REFERENCES

[1] M. Z. Win, "A unified spectral analysis of generalized time-hopping spread-spectrum signals in the presence of timing jitter," *IEEE Journal on Selected Areas in Communications*, vol. 20, no. 9, pp. 1664–1676, 2002.

[2] M. Z. Win and R. A. Scholtz, "Ultra-wide bandwidth time-hopping spread-spectrum impulse radio for wireless multiple-access communications," *IEEE Transactions on Communications*, vol. 48, no. 4, pp. 679–689, 2000.

[3] M. Z. Win and R. A. Scholtz, "Impulse radio: how it works," *IEEE Communications Letters*, vol. 2, no. 2, pp. 36–38, 1998.

[4] M. Z. Win and R. A. Scholtz, "On the robustness of ultra-wide bandwidth signals in dense multipath environments," *IEEE Communications Letters*, vol. 2, no. 2, pp. 51–53, 1998.

[5] D. Cassioli, M. Z. Win, and A. F. Molisch, "The ultra-wide bandwidth indoor channel: from statistical model to simulations," *IEEE Journal on Selected Areas in Communications*, vol. 20, no. 6, pp. 1247–1257, 2002.

[6] C.-C. Chong and S. K. Yong, "A generic statistical-based UWB channel model for high-rise apartments," *IEEE Transactions on Antennas and Propagation*, vol. 53, no. 8, pp. 2389–2399, 2005.

[7] C.-C. Chong, Y.-E. Kim, S. K. Yong, and S.-S. Lee, "Statistical characterization of the UWB propagation channel in indoor residential environment," *Wireless Communications and Mobile Computing*, vol. 5, no. 5, pp. 503–512, 2005.

[8] K. Pahlavan, X. Li, and J.-P. Mäkelä, "Indoor geolocation science and technology," *IEEE Communications Magazine*, vol. 40, no. 2, pp. 112–118, 2002.

[9] R. J. Fontana and S. J. Gunderson, "Ultra-wideband precision asset location system," in *Proceedings of IEEE Conference on Ultra Wideband Systems and Technologies*, pp. 147–150, Baltimore, Md, USA, May 2002.

[10] D. Dardari, "Pseudo-random active UWB reflectors for accurate ranging," *IEEE Communication Letters*, vol. 8, no. 10, pp. 608–610, 2004.

[11] K. Yu and I. Oppermann, "Performance of UWB position estimation based on time-of-arrival measurements," in *Proceedings of International Workshop on Ultra Wideband Systems; Joint with Conference on Ultrawideband Systems and Technologies (Joint UWBST & IWUWBS '04)*, pp. 400–404, Kyoto, Japan, May 2004.

[12] M. Z. Win and R. A. Scholtz, "Characterization of ultra-wide bandwidth wireless indoor channels: a communication-theoretic view," *IEEE Journal on Selected Areas in Communications*, vol. 20, no. 9, pp. 1613–1627, 2002.

[13] V. Lottici, A. D'Andrea, and U. Mengali, "Channel estimation for ultra-wideband communications," *IEEE Journal on Selected Areas in Communications*, vol. 20, no. 9, pp. 1638–1645, 2002.

[14] H. Boujemaa and M. Siala, "On a maximum likelihood delay acquisition algorithm," in *Proceedings of IEEE International Conference on Communications (ICC '01)*, vol. 8, pp. 2510–2514, Helsinki, Finland, June 2001.

[15] J.-Y. Lee and R. A. Scholtz, "Ranging in a dense multipath environment using an UWB radio link," *IEEE Journal on Selected Areas in Communications*, vol. 20, no. 9, pp. 1677–1683, 2002.

[16] L. Dumont, M. Fattouche, and G. Morrison, "Super-resolution of multipath channels in a spread spectrum location system," *Electronics Letters*, vol. 30, no. 19, pp. 1583–1584, 1994.

[17] X. Li and K. Pahlavan, "Super-resolution TOA estimation with diversity for indoor geolocation," *IEEE Transactions on Wireless Communications*, vol. 3, no. 1, pp. 224–234, 2004.

[18] E. R. Jàtiva and J. Vidal, "First arrival detection for positioning in mobile channels," in *Proceedings of 13th IEEE International Symposium on Personal, Indoor and Mobile Radio Communications (PIMRC '02)*, vol. 4, pp. 1540–1544, Lisbon, Portugal, September 2002.

[19] I. Maravic and M. Vetterli, "Low-complexity subspace methods for channel estimation and synchronization in ultrawideband systems," in *Proceedings of International Workshop on Ultra Wideband Systems (IWUWB '03)*, pp. 1–5, Oulu, Finland, June 2003.

[20] W. Suwansantisuk, M. Z. Win, and L. A. Shepp, "On the performance of wide-bandwidth signal acquisition in dense multipath channels," *IEEE Transactions on Vehicular Technology*, vol. 54, no. 5, pp. 1584–1594, 2005.

[21] Y. Jeong, H. You, and C. Lee, "Calibration of NLOS error for positioning systems," in *Proceedings of IEEE 53rd Vehicular Technology Conference (VTC '01)*, vol. 4, pp. 2605–2608, Rhodes, Greece, May 2001.

[22] P.-C. Chen, "A non-line-of-sight error mitigation algorithm in location estimation," in *Proceedings of IEEE Wireless Communications and Networking Conference (WCNC '99)*, vol. 1, pp. 316–320, New Orleans, La, USA, September 1999.

[23] B. Denis, J. Keignart, and N. Daniele, "Impact of NLOS propagation upon ranging precision in UWB systems," in *Proceedings of IEEE Conference on Ultra Wideband Systems and Technologies (UWBST '03)*, pp. 379–383, Reston, Va, USA, November 2003.

[24] M. P. Wylie-Green and S. S. Wang, "Robust range estimation in the presence of the non-line-of-sight error," in *Proceedings of IEEE 54th Vehicular Technology Conference (VTC '01)*, vol. 1, pp. 101–105, Rhodes, Greece, May 2001.

[25] D. Dardari, C.-C. Chong, and M. Z. Win, "Analysis of threshold-based TOA estimators in UWB channels," in *Proceedings of 14th European Signal Processing Conference (EUSIPCO '06)*, Florence, Italy, September 2006.

[26] I. Guvenc and Z. Sahinoglu, "Threshold-based TOA estimation for impulse radio UWB systems," in *Proceedings of IEEE International Conference on Ultra-Wideband (ICU '05)*, pp. 420–425, Zurich, Switzerland, September 2005.

[27] J. P. Ianniello, "Large and small error performance limits for multipath time delay estimation," *IEEE Transactions on Acoustics, Speech, and Signal Processing*, vol. 34, no. 2, pp. 245–251, 1986.

[28] H. l. Van Trees, *Detection, Estimation and Modulation Theory*, John Wiley & Sons, New York, NY, USA, 2001.

[29] M. Z. Win and R. A. Scholtz, "On the energy capture of ultrawide bandwidth signals in dense multipath environments," *IEEE Communications Letters*, vol. 2, no. 9, pp. 245–247, 1998.

Chiara Falsi received the Laurea degree in electronic engineering from the University of Florence, Florence, Italy, in 2005. From September 2004 to April 2005 she was a visiting student at Laboratory for Information and Decision Systems (LIDS), MIT, Cambridge, Mass, working on ultrawide bandwidth signal processing. She focused her research activity on channel parameters and range estimation to prepare her thesis. In 2005, after receiving the degree, she became a Fellow at the Consorzio Nazionale Interuniversitario per le Telecomunicazioni (CNIT), Florence, Italy. In collaboration with the Electronic and Communication Department (DET) of the University of Florence, she was involved in the research on security and privacy issues in wireless systems.

Davide Dardari received his Laurea degree in electronic engineering (summa cum laude) and his Ph.D. in electronic engineering and computer science from the University of Bologna, Italy, in 1993 and 1998, respectively. He has collaborated and taken a significant role in several national and European projects. From 2000 until 2005, he has been a Research Associate at the University of Bologna. He held the position of lecturer and contract Professor of electrical communications and digital transmission and telecommunications systems at the same university. Now he is Associate Professor at the University of Bologna at Cesena, Cesena (FC), Italy. During the winter of 2005 he was researching as Research Affiliate at Massachusetts Institute of Technology (MIT), Cambridge, USA. His research interests are in OFDM systems, ultra-wide bandwidth communication and localization, wireless sensor networks, wideband wireless LAN. He serves IEEE as Editor for IEEE Transactions on Wireless Communications and as TPC Member for the Wireless Communications Symposium at IEEE International Conference on Communications (ICC 2004 - ICC 2006) and PIMRC 2006. He is Cochair of the International Conference on Ultra-Wideband (ICUWB 2006) and ICC 2007 Wireless Communications Symposium.

Lorenzo Mucchi was born in Rome, Italy, in 1971. He received the Dr. Ing. Degree (Laurea) in telecommunications engineering from the University of Florence, Italy, in 1998 and the Ph.D. in telecommunications and information society in 2001. Since 2001 he has been with the Department of Electronics and Telecommunications of the University of Florence, Italy, as a Research Scientist. During the academic year 2000-2001, he spent a 12-month period of research at the Centre for Wireless Communications, University of Oulu, Oulu, Finland. His main research areas are spread spectrum techniques, adaptive filters, CDMA communication systems and satellite communications. He is actually involved in the ultra-wide-band systems and space-time codes and diversity techniques for terrestrial and satellite communications research area. He is also involved in several national and international projects. He has published a chapter in an international book and several papers (43) in international journals and conferences during his research activity. He is member of the International Association of Science and Technology for Development (IASTED) Technical Committee on Telecommunications for the term 2002-2005. He is professor of Telematics (Telecommunications and Informatics) at the University of Florence. He is also a full member of the Institute of Electrical and Electronics Engineers (IEEE).

Moe Z. Win received the B.S. degree (magna cum laude) from Texas A&M University, College Station, in 1987 and the M.S. degree from the University of Southern California (USC), Los Angeles, in 1989, both in electrical engineering. As a Presidential Fellow at USC, he received both the M.S. degree in applied mathematics and the Ph.D. degree in electrical engineering in 1998. He is an Associate Professor at the Laboratory for

Information & Decision Systems (LIDS), Massachusetts Institute of Technology. Prior to joining LIDS, he spent 5 years at AT&TResearch Laboratories and 7 years at the Jet Propulsion Laboratory. His main research interests are the application of mathematical and statistical theories to communication, detection, and estimation problems. Specific current research topics include measurement and modeling of time-varying channels, design and analysis of multiple antenna systems, ultra-wide bandwidth (UWB) communications systems, optical communications systems, and space communications systems. He has been involved actively in organizing and chairing a number of international conferences. He served as the Technical Program Chair for the IEEE Communication Theory Symposia of ICC-2004 and Globecom-2000, as well as for the IEEE Conference on Ultra Wideband Systems and Technologies in 2002, Technical Program Vice-chair for the IEEE International Conference on Communications in 2002, and the Tutorial Chair for the IEEE Semiannual International Vehicular Technology Conference in Fall 2001. He is the current chair and past secretary (2002–2004) for the Radio Communications Committee of the IEEE Communications Society. He currently serves as Area Editor for Modulation and Signal Design and Editor for Wideband Wireless and Diversity, both for IEEE Transactions on Communications. He served as the Editor for Equalization and Diversity from July 1998 to June 2003 for the IEEE Transactions on Communications, and as a Guest Editor for the 2002 IEEE Journal on Selected Areas in Communications (Special Issue on Ultra-Wideband Radio in Multiaccess Wireless Communications). He received the International Telecommunications Innovation Award from Korea Electronics Technology Institute in 2002, a Young Investigator Award from the Office of Naval Research in 2003, and the IEEE Antennas and Propagation Society Sergei A. Schelkunoff Transactions Prize Paper Award in 2003. In 2004, he was named Young Aerospace Engineer of the Year by AIAA, and garnered the Fulbright Foundation Senior Scholar Lecturing and Research Fellowship, the Institute of Advanced Study Natural Sciences and Technology Fellowship, the Outstanding International Collaboration Award from the Industrial Technology Research Institute of Taiwan, and the Presidential Early Career Award for Scientists and Engineers from the White House. He was honored with the Lifetime Achievement Award from the People of Bangladesh in 2006, and in that same year received the IEEE Eric E. Sumner Award "for pioneering contributions to ultra-wide band communications science and technology." He is an IEEE Distinguished Lecturer and elected Fellow of the IEEE, cited "for contributions to wideband wireless transmission."